

First-Principles Evaluation of the Surface Barrier for a Kohn-Sham Electron at a Metal Surface

Adolfo G. Eguiluz

Department of Physics, Montana State University, Bozeman, Montana 59717

Martin Heinrichsmeier, Andrzej Fleszar, and Werner Hanke

Physikalisches Institut, Universität Würzburg, 8700 Würzburg, Germany

(Received 1 October 1991)

The popular local-density approximation neglects long-range correlations which, in the presence of the rapid rate of change of the electron density at the surface, lead to observable effects. We evaluate the exchange-correlation potential V_{xc} for the electron gas-vacuum interface from the knowledge of the electron self-energy Σ_{xc} in the GW approximation. The electron-electron correlations built into Σ_{xc} automatically produce an imagelike surface barrier. Our result for V_{xc} is the basis of a nonlocal density-functional calculation of the electronic structure of Al(100) which yields a Rydberg series of image states from first principles.

PACS numbers: 73.20.-r, 71.10.+x

The major advances witnessed in the last two decades in the quantitative computation of ground-state properties of condensed matter systems are to a large extent due to the development of density-functional theory [1] into a powerful tool for dealing with the complicated system of 10^{23} interacting electrons.

Now, in the implementation of the density-functional scheme for a metal surface one must in principle account for the fact that the very presence of the surface introduces a source of inhomogeneity on a microscopic scale. However, in the widely used (and, for many purposes, very successful [2]) local-density approximation (LDA) [1], this feature of the surface problem is simply ignored in the treatment of the crucial electron-electron interactions.

Because of its neglect of long-range correlations, the LDA gives rise to a surface barrier with a qualitatively incorrect asymptotic behavior (exponential decay, rather than the expected *inverse power* [3]). This failure of the LDA is experimentally relevant; new surface-sensitive techniques have produced a wealth of data on observables and processes influenced by the image tail of the surface barrier, such as binding energies and lifetimes of image potential-bound surface states [4], tunneling currents in the scanning-tunneling microscope [5], resonant-tunneling rates for ion-surface collisions [6], etc.

In this Letter we report a first-principles evaluation of the exchange-correlation potential (V_{xc}) for the electron gas-vacuum interface. We proceed by solving an exact integral equation relating V_{xc} and the electron self-energy. The main physical ingredients of the self-energy, namely, its energy dependence and long-range correlations, and their interplay with the extreme inhomogeneity

of the surface environment, are treated exactly within the GW approximation [7]. As a consequence we obtain a surface barrier which is imagelike in the vacuum.

Our result for V_{xc} is applied in two contexts. (i) We elucidate the physics of the many-body surface barrier experienced by a Kohn-Sham (KS) electron (i.e., an "electron" described by an eigenfunction of the KS equation) for distances relevant to many experiments [4-6]. We show that while Coulomb correlation is indeed responsible for the z^{-1} limit of the barrier, the position of the image plane appropriate for a KS electron is not the same as the one appropriate for a classical test charge. (ii) We establish a "nonlocal" relation between V_{xc} and the electron density which is the basis of a calculation of the electronic structure of Al(100). The long-range correlations responsible for the existence of the image tail of the surface barrier automatically produce a Rydberg series of image states [4]. These states (and the physics behind them) are beyond the realm of the LDA.

In density-functional theory [1,2] the many-body contribution to the self-consistent surface barrier is given by the exchange-correlation potential $V_{xc}(\mathbf{x})$, defined by the equation $V_{xc}(\mathbf{x}) = \delta E_{xc}[n]/\delta n(\mathbf{x})$, where $E_{xc}[n]$ is the exchange and correlation energy functional [1], and $n(\mathbf{x})$ is the electron number density. The exact form of $E_{xc}[n]$ is unknown; several functional forms have been contrived in order to enforce the presence of an image tail in an *ad hoc* way [8-10].

In our work we take a different approach, i.e., we do not invoke the above definition at all; rather, we define $V_{xc}(\mathbf{x})$ through the following exact integral equation, which relates it to the electron self-energy $\Sigma_{xc}(\mathbf{x}, \mathbf{x}'|E)$ of many-body perturbation theory [11,12]:

$$\int d^3x_1 V_{xc}(\mathbf{x}_1) \int dE g_0(\mathbf{x}, \mathbf{x}_1|E) g(\mathbf{x}_1, \mathbf{x}|E) = \int d^3x_1 \int d^3x_2 \int dE g_0(\mathbf{x}, \mathbf{x}_1|E) \Sigma_{xc}(\mathbf{x}_1, \mathbf{x}_2|E) g(\mathbf{x}_2, \mathbf{x}|E), \quad (1)$$

where g is the quasiparticle Green's function, and g_0 is the Green's function for the KS Hamiltonian. Note that while V_{xc} is by definition a local, energy-independent potential, and g_0 describes the propagation of a KS electron in the presence of this potential, a "real" electron (quasiparticle) propagates (via g) in the presence of the nonlocal, energy-dependent self-energy.

The state-of-the-art first-principles computation of the electron self-energy in solids [13,14] is the GW approximation due to Hedin [7],

$$\Sigma_{xc}(\mathbf{x}_1, \mathbf{x}_2|E) = \frac{i}{2\pi} \int dE' e^{iE'\eta} g(\mathbf{x}_1, \mathbf{x}_2|E + E') W(\mathbf{x}_1, \mathbf{x}_2|E'), \quad (2)$$

which is the first term in an expansion of the self-energy in powers of the dynamically screened electron-electron interaction $W(\mathbf{x}_1, \mathbf{x}_2|E)$, defined by the equation (written symbolically) [7]

$$W = v + v\chi_T v, \quad (3)$$

where v is the bare Coulomb interaction, and χ_T is the time-ordered density response function, which satisfies the integral equation [7] $\chi_T = \tilde{\chi} + \tilde{\chi}v\chi_T$, where $\tilde{\chi}$ is the irreducible polarizability. In the present work we set $\tilde{\chi} = \chi^0$, where χ^0 is electron-hole pair bubble. Thus we neglect, e.g., excitonic effects (ladder diagrams).

A few technical details about our method are in order. (i) Since the Green's function g_0 depends on V_{xc} , Eq. (1) poses a self-consistency problem, which we solved by iteration. Wave functions and energy eigenvalues with which to compute "updated" Σ_{xc} and g_0 are obtained by feeding the solution of Eq. (1) into the KS equation. [One or two iterations are required for full convergence of the tail of the potential, the near-surface region requiring just a single solution.] (ii) Following standard practice [12], we have set $g_0 = g$ throughout. (iii) The time-ordered response function χ_T is expressed in terms of its retarded counterpart χ_R via a Lehmann representation [7]. χ_R is computed for a jellium slab *without imposing any restrictions on the rate of spatial change of the electron density at the surface* [15]. (The slab thickness used corresponds to four or more Fermi wavelengths.) The full energy dependence of χ_R was kept; we did not introduce a plasmon-pole approximation [14] because at the surface (unlike the bulk), Landau damping plays a role even for small wave vectors—a reflection of the breakdown of translational invariance in the direction normal to the surface. (iv) The energy integral involving χ_R is performed (by Gaussian quadrature) upon distorting the contour so that it runs over the imaginary axis. (v) The electron density decays to zero in the vacuum, and this renders the kernel of Eq. (1) singular. Furthermore, the

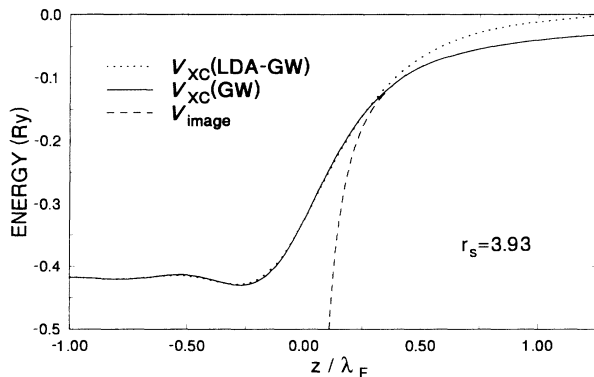


FIG. 1. $V_{xc}(z)$ at a simple metal surface for $r_s = 3.93$ (for which $\lambda_F = 12.9$ a.u.). The solid curve is the solution of Eq. (1) with use of the GW approximation for Σ_{xc} , and the dotted curve is the corresponding LDA potential [17]. The dashed curve is the image potential $V_{im}(z) = -e^2/4(z - z_0)$.

integral equation is *homogeneous*, which makes it numerically very unstable. Use of the singular-value decomposition method proved effective [16].

Figure 1 shows a representative solution of Eq. (1) for (the electron-gas parameter) $r_s = 3.93$. That solution is compared with the corresponding LDA potential [17] and with the image potential $V_{im}(z) = -e^2/4(z - z_0)$, where z is the coordinate normal to the surface and z_0 is the position of the effective image plane [18,19]. The key feature of our result is that $V_{xc}(z)$ becomes imagelike outside the surface. This is an important improvement over LDA in the context of experiments whose interpretation is linked to the existence of the image tail of the barrier [4-6].

The physics of the surface barrier is best discussed with reference to Fig. 2, in which we show the solutions of Eq. (1) that obtain from the use of the Hartree-Fock (Σ_{HF}) and Coulomb-correlation (Σ_c) self-energies, which originate, respectively, from the first and second terms in Eq. (3). These solutions are labeled $V_x(\Sigma_{HF})$ and $V_c(\Sigma_c)$. ($\Sigma_{xc} = \Sigma_{HF} + \Sigma_c$; in Fig. 2 we have set $\Sigma_{GW} = \Sigma_{xc}$.) It is apparent that the classical-image limit of the surface barrier, $V_{xc}(z) \rightarrow -e^2/4z$, is due to the Coulomb-correlation effect present in Σ_c . *Thus this limit is "universal,"* being the same for a KS electron and for a classical test charge. [This conclusion confirms earlier statements of Almladh and von Barth [20] and Sham [21]; it disagrees with the conclusions of Harbola and Sahni [22], who have equated $V_{xc}(z)$ for large z with the work performed against the bare-exchange hole [23].]

From the potentials shown in Fig. 2 we conclude that the position of the effective image plane includes a significant contribution from the exchange process [which is why the full $V_{xc}(z)$ merges with $V_{im}(z)$ much closer to the surface than the correlation-only potential V_c does]. In fact, we have shown numerically that $V_x(z) \rightarrow -a/z^2$, the coefficient a giving the contribution to z_0 from exchange. Clearly then, *the image-plane position that governs the barrier that self-binds a KS electron differs from its counterpart for a test charge.* Thus, the z_0 for a

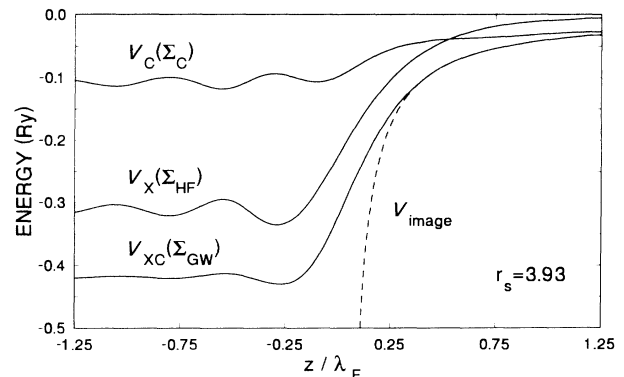


FIG. 2. Solution of Eq. (1) for three approximations for the self-energy: Σ_{HF} (Hartree-Fock), Σ_c (correlation), and Σ_{GW} (sum of the previous two).

KS electron is not (contrary to statements made in the literature [9]) the one that arises in the context of the linear response of the surface to an external, uniform electric field [3].

Quantitatively we have that, e.g., for $r_s=2.07$, the image-plane position extracted from the image tail of V_{xc} [18] is $z_0=0.72\pm 0.1$ a.u. (measured from the jellium edge), while from linear response in LDA-GW [17], $z_0=1.49$ a.u. [24]. The nonlocal effects alter the linear-response value very little. These issues, including the effects of the crystal structure, will be discussed in detail elsewhere [25].

Starting from the position of the first Friedel peak of the density, and moving out into the vacuum, we have constructed, by a point-by-point "tabulation" of the solution of Eq. (1) and the electron density self-consistent with it, a one-to-one relation between V_{xc} and n to be symbolized as $V_{xc}(r_s;n^{1/3})$. The appeal of this relation, which derives implicitly from a functional $E_{xc}[n]$ containing the physics of the nonlocal self-energy, is that Eq. (1) has been solved once and for all for each value of r_s . The same $V_{xc}(z)$ shown in Fig. 1 can now be obtained directly (as we have checked explicitly) from the self-consistent solution of the KS equation in the presence of our $V_{xc}(r_s;n^{1/3})$ relation (matched to the LDA at the first Friedel peak). This represents an enormous simplification relative to solving Eq. (1).

A detailed parametrization of our $V_{xc}(r_s;n^{1/3})$ relation will be presented elsewhere for r_s values in the metallic range [25]. Here we report its first application to a density-functional calculation of the electronic structure of Al(100), performed in a periodic-slab geometry, with use of a plane-wave basis set, and *ab initio* norm-

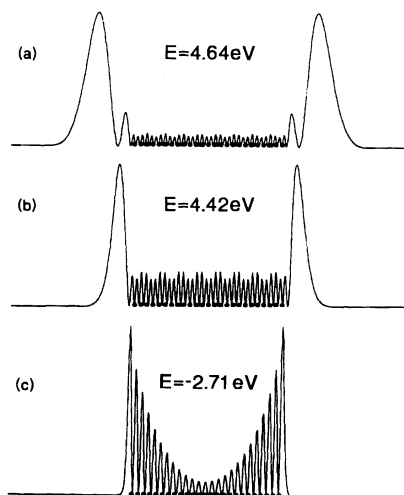


FIG. 3. Squares of three of the eigenfunctions for Al(100) (averaged over the surface plane) at $\bar{\Gamma}$, obtained in the presence of the nonlocal effects discussed in the text. The energy eigenvalues are measured from the Fermi level; the vacuum level is at 4.82 eV. (a) $n=2$ image state (resonance). (b) $n=1$ image state (resonance). (c) Surface state in the gap. Circles: positions of the atomic planes.

conserving pseudopotentials [26]. Since the new physics included in our method is related to the existence of image states whose wave functions are localized many atomic units outside the surface, a large vacuum gap between consecutive slabs must be utilized. Furthermore, in order to separate the members of the Rydberg series of image states, the physical slab must be at least 25 atomic layers thick. Both requirements translate into the use of a very large unit cell. [In the self-consistency procedure for this three-dimensional calculation the "nonlocal" V_{xc} is matched to V_{xc} in the LDA in the vicinity of the nominal jellium edge. The precise point where the matching is done is not important, a consequence of the result (see Fig. 1) that the nonlocal and LDA potentials are very close to each other over a sizable interval about the jellium edge.]

In Fig. 3 we show the squares of three of the eigenfunctions at $\bar{\Gamma}$ (averaged over the plane of the surface). The energy position of the "conventional" surface state [3(c)] is in very good agreement with the photoemission observations of Levinson, Greuter, and Plummer [27]. The states at 4.42 and 4.64 eV above E_F owe their existence to the image tail of the barrier. This statement is substantiated in Fig. 4, which shows a weighted density of states (DOS) near the vacuum level, for both nonlocal and LDA [17] calculations. Both calculations give the same results for states such as that in Fig. 3(c), but the LDA entirely misses the Rydberg series. We emphasize that eigenstates of the form of those in Figs. 3(a) and 3(b) occur over a finite energy range; *they correspond to resonances*. [Note how state (c) decays monotonically into the bulk, unlike the resonances.] Finally, we note that although no experimental data have been reported for the image states of Al(100), the binding energy of the $n=1$ resonance (Fig. 4) compares favorably with the location of the image-state peak (~ 0.45 eV) in the inverse-photoemission data of Heskett *et al.* [28] for Al(111).

The direct solution of Eq. (1) for a real metal will be

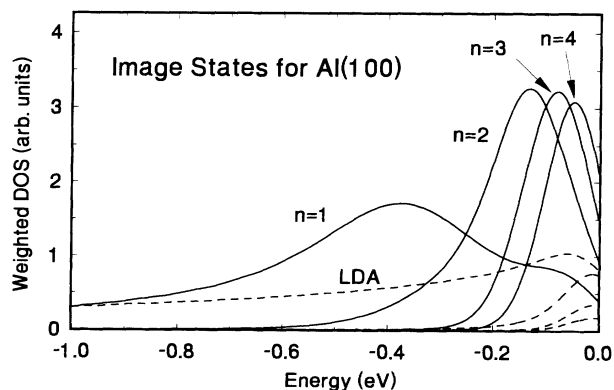


FIG. 4. Weighted DOS near the vacuum level for Al(100) at $\bar{\Gamma}$. (See text.) The solid curves correspond to the image-state resonances. The dashed curves are the corresponding LDA results [17]. Energies are measured from the vacuum level.

attempted in future work. Such a calculation would produce a V_{xc} in which the (beyond-the-LDA) "bulk" many-body effects of the electronic inhomogeneity due to the ion cores would be treated together with the effects investigated in the present work, which are inherent to the presence of the surface [10]. (Since the LDA is known to hold qualitatively in the bulk, the former effects are not as dramatic as the ones discussed in this work.)

In summary, we have evaluated from first principles the surface barrier for a KS electron at the electron gas surface from the knowledge of the electron self-energy in the GW approximation. We have developed a scheme for carrying out nonlocal density-functional calculations with the same ease as LDA-based calculations. This scheme includes the combined effects of long-range electron-electron correlations and the rapid rate of change of the electron density at the surface. The scheme has been tested successfully for Al(100); it yields a Rydberg series of image states on the same footing with conventional (crystal-termination) surface states. A similar calculation is under way for Pd(111) [29].

We thank E. K. U. Gross for a critical reading of the manuscript. The work of A.G.E. was supported in part by NSF Grant No. DMR 86-038920, by MONTS Grant No. 196504, and by the San Diego Supercomputer Center. The work of A.F. was supported by the DFG under Contract No. HA 1537/1-4, and that of M.H. by the BMFT under Contract No. 03-HA2WUE. A.G.E. and W.H. acknowledge the support of NATO.

- [1] P. Hohenberg and W. Kohn, *Phys. Rev.* **136**, B864 (1964); W. Kohn and L. J. Sham, *Phys. Rev.* **140**, A1133 (1965).
- [2] For recent developments, see *Density Functional Theory of Many-Fermion Systems*, edited by S. B. Trickey (Academic, New York, 1990), and R. M. Dreizler and E. K. U. Gross, *Density Functional Theory: An Approach to the Quantum Many-Body Problem* (Springer-Verlag, Berlin, 1990).
- [3] N. D. Lang and W. Kohn, *Phys. Rev. B* **7**, 3541 (1973).
- [4] P. M. Echenique and J. B. Pendry, *Prog. Surf. Sci.* **32**, 11 (1990); M. Donath *et al.*, *Phys. Rev. B* **41**, 5509 (1990); F. J. Himpsel, *Phys. Rev. B* **43**, 13394 (1991); N. V. Smith, *Rep. Prog. Phys.* **51**, 1227 (1988).
- [5] G. Binnig *et al.*, *Phys. Rev. B* **30**, 4816 (1984); B. N. J. Persson and A. Baratoff, *ibid.* **38**, 9616 (1988); A. A. Lucas *et al.*, *ibid.* **37**, 10708 (1988); G. Doyen *et al.*, *Appl. Phys. A* **51**, 281 (1990).
- [6] P. Nordlander, and J. C. Tully, *Surf. Sci.* **211/212**, 207 (1989).
- [7] L. Hedin and S. Lundqvist, in *Solid State Physics*, edited by H. Ehrenreich, F. Seitz, and D. Turnbull (Academic, New York, 1969), Vol. 23, p. 1.
- [8] S. Ossicini, C. M. Bertoni, and P. Gies, *Europhys. Lett.* **1**, 661 (1986); O. Gunnarsson and R. O. Jones, *Phys. Scr.* **21**, 394 (1980).
- [9] P. A. Serena, J. M. Soler, and N. García, *Phys. Rev. B* **34**, 6767 (1986).
- [10] The functional proposed by D. C. Langreth and M. J. Mehl [*Phys. Rev. Lett.* **47**, 446 (1981)] does not give rise to an imagelike surface barrier. Their method accounts approximately for the "bulk" electronic many-body effects brought about by the presence of the ion cores.
- [11] L. J. Sham and M. Schlüter, *Phys. Rev. Lett.* **51**, 1888 (1983).
- [12] R. W. Godby, M. Schlüter, and L. J. Sham, *Phys. Rev. Lett.* **56**, 2415 (1986); *Phys. Rev. B* **37**, 10159 (1988); W. Hanke and L. J. Sham, *ibid.* **38**, 13361 (1988).
- [13] G. Strinati, H. J. Mattausch, and W. Hanke, *Phys. Rev. B* **25**, 2867 (1982).
- [14] M. S. Hybertsen and S. G. Louie, *Phys. Rev. B* **38**, 4033 (1988); J. E. Northrup, M. S. Hybertsen, and S. G. Louie, *Phys. Rev. Lett.* **66**, 500 (1991).
- [15] A. G. Eguiluz, *Phys. Rev. B* **31**, 3305 (1985); *Phys. Scr.* **36**, 651 (1987).
- [16] W. H. Press *et al.*, *Numerical Recipes* (Cambridge Univ. Press, Cambridge, 1986).
- [17] For the homogeneous electron gas, the solution of Eq. (1) is given by $V_{xc} = \Sigma_{xc}(k = k_F; E = E_F)$; the LDA results we compare with are obtained from this (exact) result, with use of the bulk GW self-energy. (The GW yields a V_{xc} that differs from the value extracted from the Ceperley and Alder Monte Carlo calculation [*Phys. Rev. Lett.* **45**, 566 (1980)] by about 5% for small r_s .)
- [18] Because of the instability of the integral equation the tail of the barrier is affected (on a finer scale of energies than the one used in Figs. 1 and 2) by numerical inaccuracies in the computation of the right-hand side of Eq. (1). This limits the accuracy of the z_0 extracted from the tail.
- [19] A. G. Eguiluz and W. Hanke, *Phys. Rev. B* **39**, 10433 (1989).
- [20] C. O. Almbladh and U. von Barth, *Phys. Rev. B* **31**, 3231 (1985).
- [21] L. J. Sham, *Phys. Rev. B* **32**, 3876 (1985).
- [22] M. K. Harbola and V. Sahni, *Phys. Rev. B* **39**, 10437 (1989).
- [23] The ultimate reason behind this discrepancy between the method of Ref. [22] and the present work is not immediately obvious, and deserves further investigation.
- [24] For completeness we note that for $r_s = 2.0$ the method of Ossicini, Bertoni, and Gies [8] gives $z_0 = 0.85$ a.u. (extracted from the tail of V_{xc}), whereas the linear-response (LDA) value of Lang and Kohn [3] is $z_0 = 1.60$ a.u.
- [25] A. G. Eguiluz, M. Heinrichsmeier, A. Fleszar, and W. Hanke (to be published).
- [26] G. B. Bachelet, D. R. Hamann, and M. Schlüter, *Phys. Rev. B* **26**, 4199 (1982).
- [27] H. J. Levinson, F. Greuter, and E. W. Plummer, *Phys. Rev. B* **27**, 727 (1983).
- [28] D. Heskett *et al.*, *Phys. Rev. B* **37**, 10387 (1988).
- [29] In this calculation, to be reported elsewhere, an effective value of r_s must be defined. In the case of Al we averaged V_{xc} over the unit cell, and extracted r_s from the LDA- GW [17] V_{xc} vs n relation; this procedure yielded $r_s = 2.07$. The (three-dimensional) surface barrier, determined for this r_s value, joins smoothly with the bulk V_{xc} potential. We are currently trying this and other procedures for d -electron metals such as Pd.